

## Supporting Information for

# Insights into the Origin of Aggregation Enhanced Emission of 9,10-distyrylanthracene Derivatives

Jibo Zhang,<sup>a,†</sup> Suqian Ma,<sup>a,†</sup> Honghua Fang,<sup>b</sup> Bin Xu<sup>\*,a</sup>, Hongbo Sun,<sup>b</sup> Im Chan,<sup>c,d</sup> and Wenjing Tian<sup>\*,a</sup>

<sup>a</sup>. State Key Laboratory of Supramolecular Structure and Materials, Jilin University Qianjin Street No. 2699, Changchun 130012, P. R. China.

<sup>b</sup>. State Key Laboratory on Integrated Optoelectronics, Jilin University, Qianjin Street No. 2699, Changchun 130012, P.R. China.

<sup>c</sup>. Konkuk University–Fraunhofer Institute for Solar Energy Systems Next Generation Solar Cell Research Center (KFnSC), Konkuk University, 120 Neungdong-ro, Gwangjin-gu, Seoul 143-701, Republic of Korea

<sup>d</sup>. Department of Chemistry, Konkuk University, 120 Neungdong-ro, Gwangjin-gu, Seoul 143-701, Republic of Korea

## Table of Contents

1. General Information.
2. **Scheme S1.** Molecular structures of AnPHZ2 and AnPHZ4.
3. **Figure S1.** PL and absorption spectra of the derivatives in different solvents.
4. **Figure S2.** Schematic drawing of the dihedral angles.
5. **Figure S3.** PL spectra of the derivatives in 2-methyltetrahydrofuran at 77K.
6. **Figure S4.** Calculated dihedral angles of DSA and BDPVA in the excited state.
7. **Figure S5.** TCSPC data of the derivatives in tetrahydrofuran.
8. **Figure S6.** TCSPC data of the derivatives in PMMA films.
9. **Figure S7.** TCSPC data of the derivatives in single crystals.
10. Crystal data and structure refinements of the crystals.

## 1. General information

All reagents and solvents were purchased from Aldrich Chemical Co. as used as received without further purification except for the notifications. UV-vis absorption spectra were recorded on a Shimadzu UV-3100 spectrophotometer. Photo luminescence spectra were collected on a Shimadzu RF-5301PC spectrophotometer and Maya 2000Pro optical fiber spectrophotometer. The fluorescence quantum yields of samples in solutions were estimated by using quinine sulfate in 0.1M sulphuric acid as a standard. The final value of quantum yield was obtained from the average of three measurements with different absorbance in the range between 0.05 and 0.10. The molecule geometries were fully optimized by the density functional theory (DFT) method with the Becke three-parameter hybrid exchange and the Lee-Yang-Parr correlation functional (B3LYP) and 6-31G\* basis set using the Gaussian 03 software package. The crystals are prepared by solvents diffusion process. The diffraction data of crystals were collected on a Rigaku RAXIS-PRID diffractometer using the  $\omega$ -scan mode with graphite-monochromator Mo-K $\alpha$  radiation. The structures were solved with direct methods using SHELXTL and refined with full-matrix least-squares on F<sup>2</sup>. Non-hydrogen atoms were refined anisotropically. The positions of hydrogen atoms were calculated and refined isotropically.

The fluorescence lifetime was performed by the time-correlated single-photon counting (TCSPC) system under right-angle sample geometry using *mini- $\tau$*  Miniature Fluorescence Lifetime Spectrometer (Edinburgh Instruments). A 405 nm picosecond diode laser (Edinburgh Instruments EPL-405, repetition rate 5 MHz, 52.6ps) was used to excite the samples. The concentration of solution was kept at  $1 \times 10^{-5}$  mol L<sup>-1</sup>. Ultrafast time-resolved emission was

measured by the femtosecond fluorescence upconversion method.<sup>1-2</sup> A Nd:YVO laser (Millennia, Spectra Physics) was used to pump a Ti: sapphire laser (Tsunami, Spectra Physics). Its output seeds a regenerative amplifier (RGA, Spitfire, Spectra Physics). The output of the amplifier of 1.5 mJ pulse energy, 100 fs pulse width, at 800 nm wavelength is split into two equal parts. The second harmonic of one beam was focused in the sample as excitation. The resulting fluorescence was collected and focused onto a 1 mm thick BBO crystal with a cutting angle of 35°. The other part of the RGA output was sent into an optical delay line and served as the optical gate for the upconversion of the fluorescence. The generated sum frequency light was then collimated and focused into the entrance slit of a 300 mm monochromator. A UV-sensitive photomultiplier tube 1P28 (Hamamatsu) was used to detect the signal. The electrical signal from the photomultiplier tube was summed by a digital oscilloscope. The relative polarization of the excitation and the gating beams was set to the magic angle. The fwhm of instrument response function was about 500 fs. All the measurements were performed at room temperature. The femtosecond transient absorption spectroscopy was performed under similar condition. A Nd:YVO laser (Millennia, Spectra Physics) was used to pump a Ti: sapphire laser (Tsunami, Spectra Physics). Its output seeds a regenerative amplifier (RGA, Spitfire, Spectra Physics). The output of the amplifier of 1.5 mJ pulse energy, 100 fs pulse width, at 800 nm wavelength is split into two equal parts. One of them (800 nm) was then used to generate a white light continuum as the probe beam. The other was either used to pump OPA to generate excitation pulse at 345 nm or sent to a 1 mm thick BBO to get the double frequency of 400 nm excitation pulses, which were then sent to a delay line and modulated by a synchronized optical chopper (Newport Model 75160) with a frequency of 125 Hz as the pump beam to excite the sample. Time-resolved transient absorption spectra were recorded

with a highly sensitive spectrometer (Avantes AvaSpec-204814). The dynamics traces were obtained by controlling the relative delay between the pump and the probe pulses with a stepper motor-driven optical delay line (Newport M-ILS250CC). The relative polarization of the excitation and the probe beams was set to the magic angle for all the measurements. The group velocity dispersion of the whole experimental system was compensated by a chirp program. The intensities of the pump pulses were measured with a laser power meter (Sanwa LP1). The excitation spot is about 300  $\mu\text{m}$  in diameter. All the measurements were performed at room temperature.

The synthesis of the derivatives could be found elsewhere in the literatures as follow:

BDPVA: An Organic Luminescent Molecule: What Will Happen When the “Butterflies” Come Together? *Adv. Mater.* **2014**, *26*, 739-745.

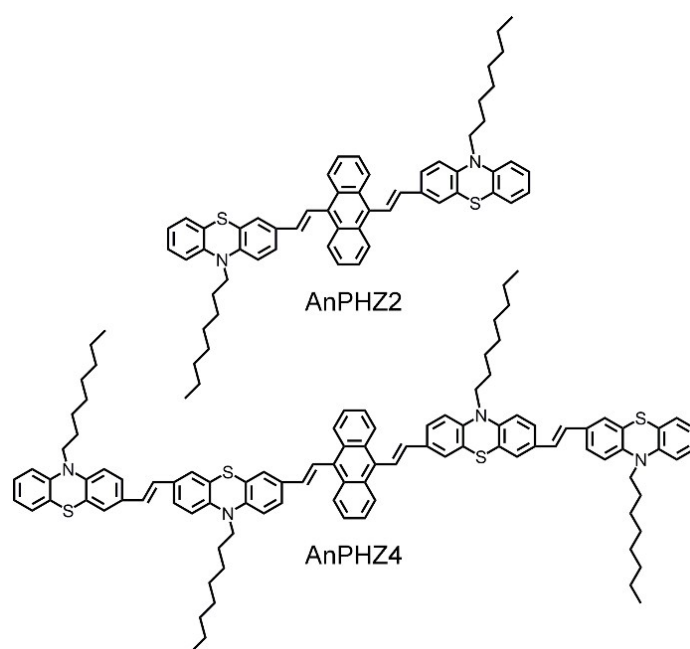
BP2VA: Piezochromic Luminescence Based on the Molecular Aggregation of 9,10-Bis((E)-2-(pyrid-2-yl)vinyl)anthracene. *Angew. Chem. Int. Ed.* **2012**, *51*, 10782-10785.

DSA: Aggregation-Induced Emission in the Crystals of 9,10-Distyrylanthracene Derivatives: The Essential Role of Restricted Intramolecular Torsion. *J. Phys. Chem. C* **2009**, *113*, 9892-9899.

BMOSA: Aggregation-Induced Emission in the Crystals of 9,10-Distyrylanthracene Derivatives: The Essential Role of Restricted Intramolecular Torsion. *J. Phys. Chem. C* **2009**, *113*, 9892-9899.

BTVA: Preparation of 9,10-divinylanthracene derivatives and application in organic light emitting diodes. CN 101279888 (2008).

2. Molecular structures of AnPHZ2 and AnPHZ4.



**Scheme S1.** Molecular structure of AnPHZ2 and AnPHZ4.

3. PL and absorption spectra of the derivatives in different solvents.

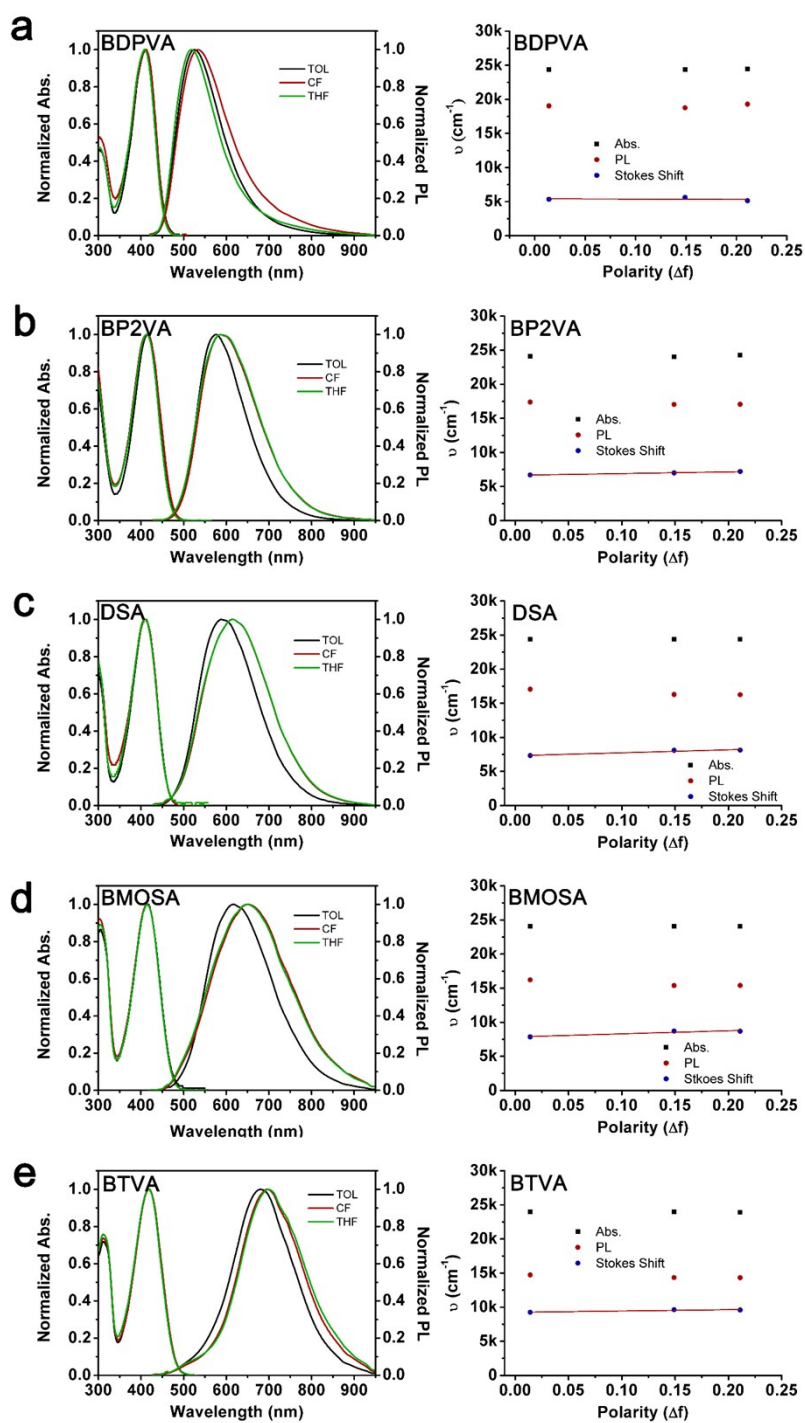


**Figure S1.** Absorption and fluorescence spectra of the derivatives (a: BDPVA, b: BP2VA, c: DSA, d: BMOSA, e: BTVA) in different solvents.

3. Schematic drawing of the dihedral angles

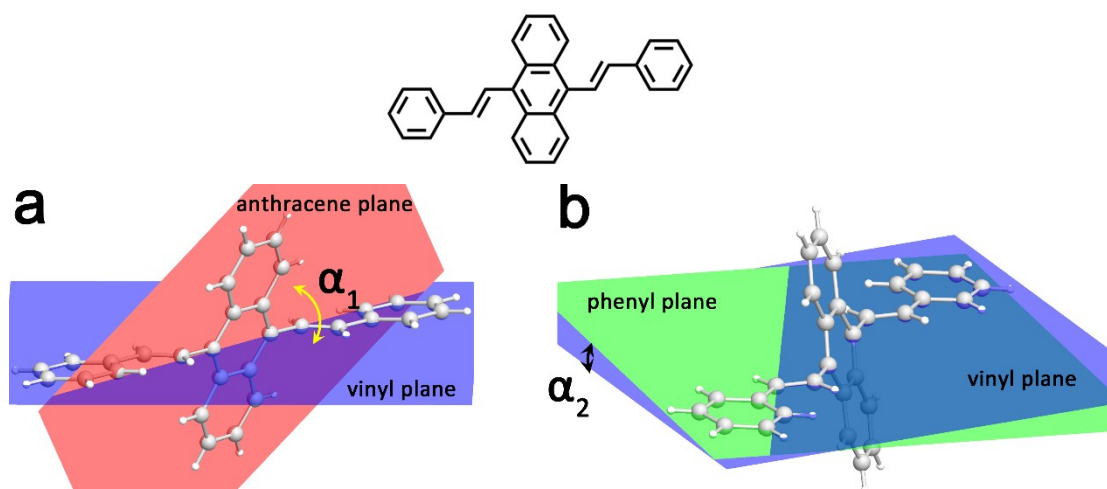


Figure S2. Schematic drawing of the dihedral angles

4. PL spectra in 2-methyltetrahydrofuran at 77K

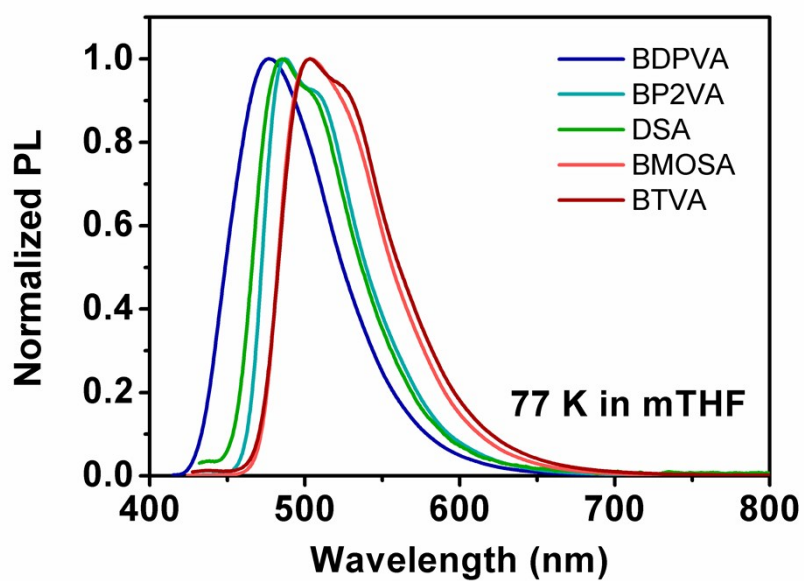
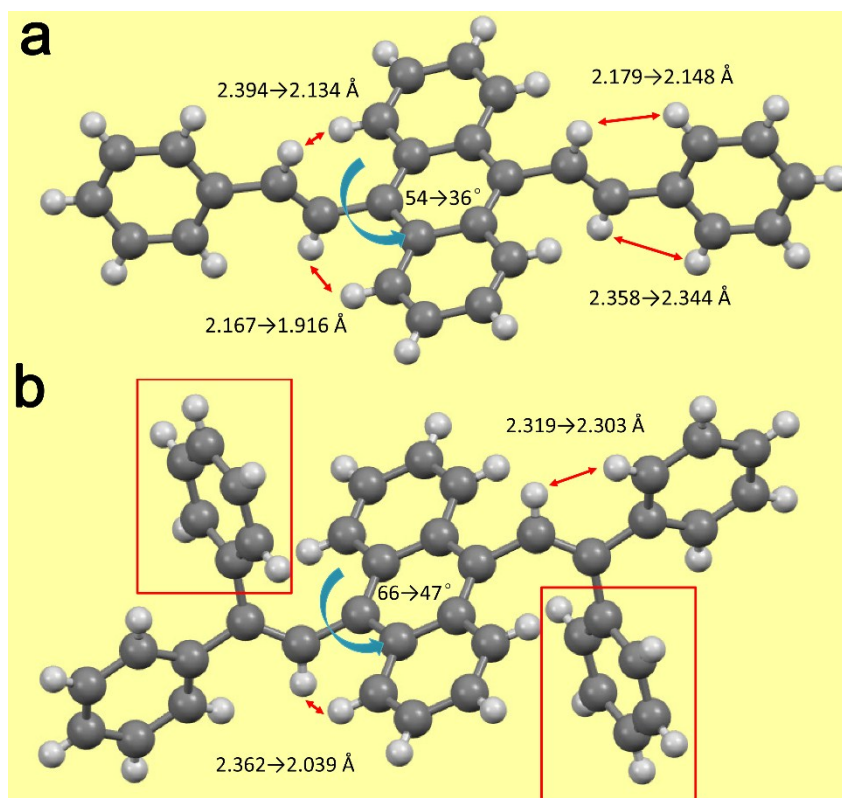


Figure S3. PL spectra of the derivatives in 2-methyltetrahydrofuran at 77K.

5. Calculated dihedral angles of DSA and BDPVA in the excited state



**Figure S4.** Calculated dihedral angles of (a) DSA and (b) BDPVA in the excited state. Blue arrow indicates the dihedral angle between the anthracene and vinyl planes.

6. TCSPC data of the derivatives in tetrahydrofuran.

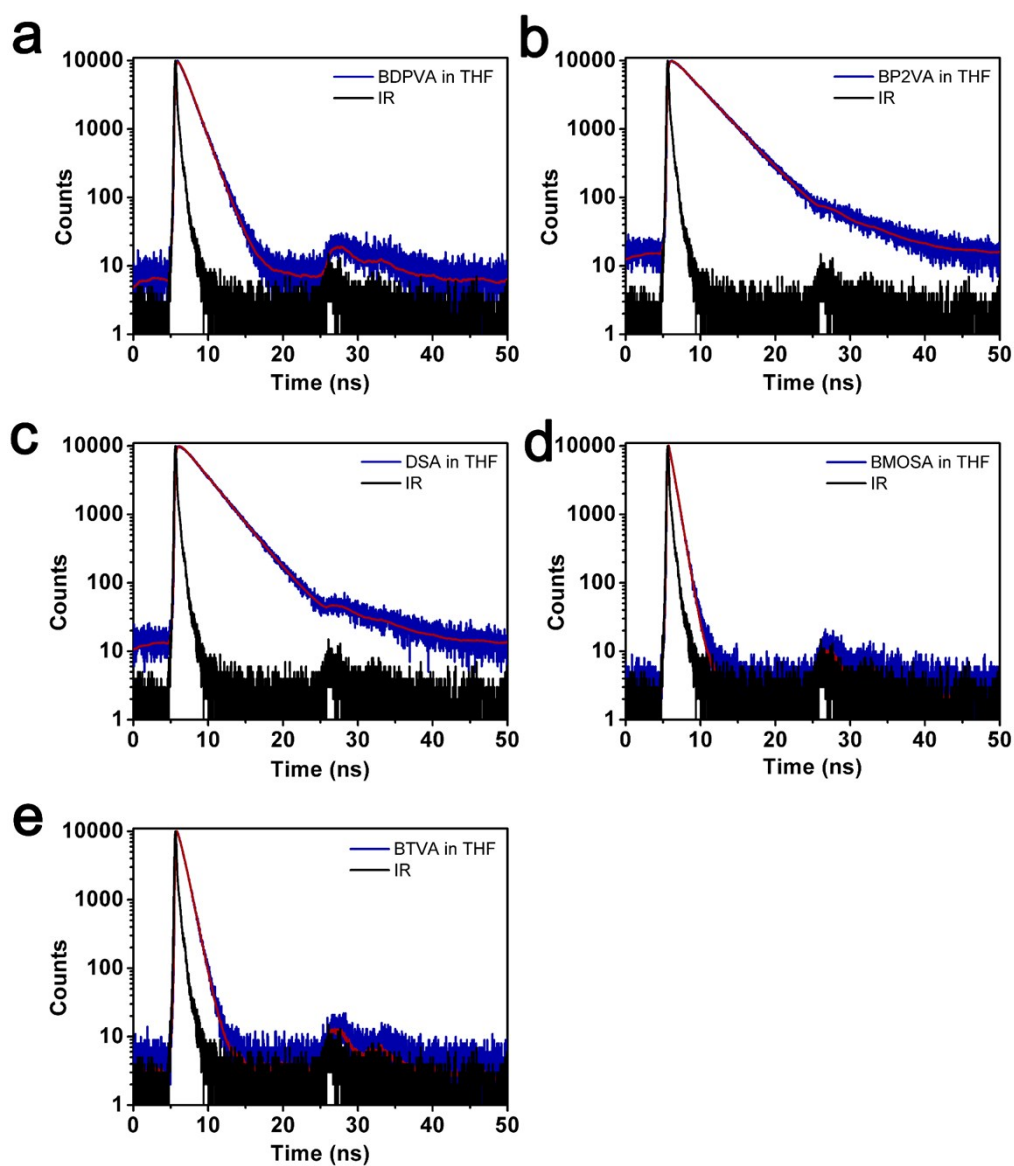


**Figure S5.** Time-resolved peak fluorescence of the derivatives (a: BDPVA, b: BP2VA, c: DSA, d: BMOSA, e: BTVA) in tetrahydrofuran (IR: instrument response, fitted line is in red).

7. TCSPC data of the derivatives in PMMA films.

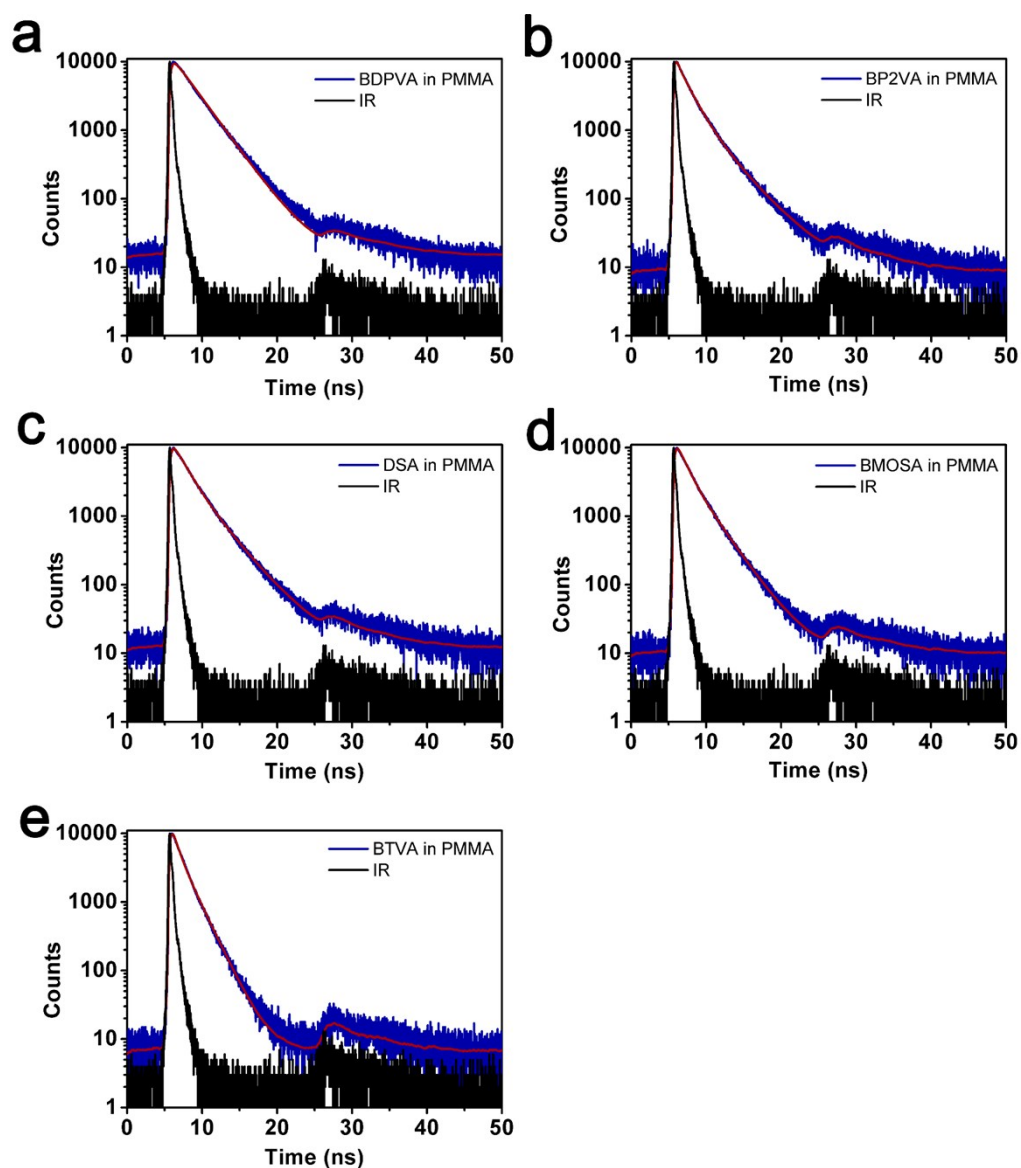


**Figure S6.** Time-resolved peak fluorescence of the derivatives in PMMA films (IR: instrument response, fitted line is in red).

8. TCSPC data of the derivatives in single crystals.

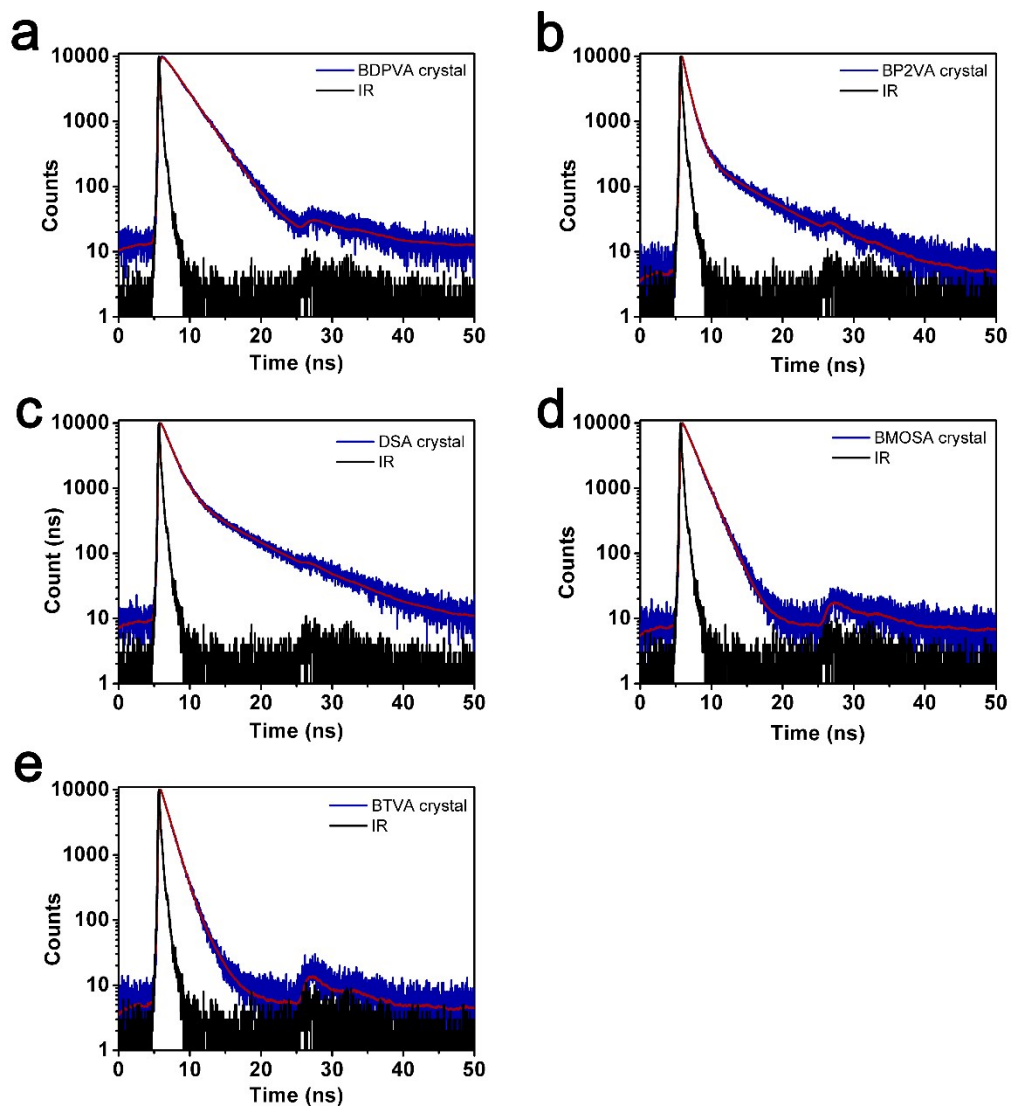


**Figure S7.** Time-resolved peak fluorescence of the derivatives in single crystals (IR: instrument response, fitted line is in red).

## 9. Crystal data and structure refinements of the crystals

	BDPVA	BP2VA	DSA
empirical formula	C <sub>42</sub> H <sub>30</sub>	C <sub>28</sub> H <sub>20</sub> N <sub>2</sub>	C <sub>30</sub> H <sub>22</sub>
formula wt	534.66	384.46	382.48
<i>T</i> , K	293(2)	293(2)	293(2)
crystal system	Triclinic	Monoclinic	Monoclinic,
space group	P-1	C2/c	P2(1)/n
<i>a</i> , Å	10.381(2)	16.017(3)	5.2500(10)
<i>b</i> , Å	11.290(2)	8.1213(16)	9.4591(19)
<i>c</i> , Å	14.078(3)	15.553(3)	20.734(4)
<i>α</i> , deg	68.76(3)	90	90
<i>β</i> , deg	80.19(3)	91.49(3)	90.70(3)
<i>γ</i> , deg	71.01(3)	90	90
<i>V</i> , Å <sup>3</sup>	1451.7 (5)	2022.4(7)	1029.6(4)
<i>Z</i>	2	4	2
F(000)	564	808	404
density, Mg/m <sup>3</sup>	1.223	1.263	1.234
Crystal size, mm	0.070×0.086×0.588	0.39×0.26×0.18	0.19×0.12×0.11
Absorption coefficient, mm <sup>-1</sup>	0.069	0.074	0.070
<i>θ</i> range, deg	3.10-27.47	3.09-27.48	3.65-27.46
no. of reflns collected	14387	9726	9805
no. of unique reflns	6591	2320	2348
<i>R</i> (int)	0.0705	0.0277	0.0633
Good-of-fit on F <sup>2</sup>	0.987	1.071	1.074
<i>R</i> <sub>1</sub> [ <i>I</i> > 2σ( <i>I</i> )]	0.0754	0.0376	0.0736
<i>wR</i> <sub>2</sub> [ <i>I</i> > 2σ( <i>I</i> )]	0.1504	0.1075	0.2221
<i>R</i> <sub>1</sub> (all data)	0.1820	0.0537	0.1268
<i>wR</i> <sub>2</sub> (all data)	0.1986	0.1158	0.2460

	BMOSA	BTVA
empirical formula	C <sub>32</sub> H <sub>26</sub> O <sub>2</sub>	C <sub>26</sub> H <sub>18</sub> S <sub>2</sub>
formula wt	442.53	394.52
<i>T</i> , K	293(2)	293(2)
crystal system	Triclinic	Monoclinic
space group	P-1	P2(1)/c
<i>a</i> , Å	6.9598(14)	5.641(3)
<i>b</i> , Å	8.8751(18)	9.315(7)
<i>c</i> , Å	10.465(2)	19.216(9)
$\alpha$ , deg	101.50(3)	90
$\beta$ , deg	99.17(3)	103.97
$\gamma$ , deg	105.19(3)	90
<i>V</i> , Å <sup>3</sup>	595.8(2)	979.8(10)
<i>Z</i>	1	2
F(000)	234	412
density, Mg/m <sup>3</sup>	1.233	1.337
Crystal size, mm	0.63×0.28×0.10	0.28×0.12×0.10
Absorption coefficient, mm <sup>-1</sup>	0.075	0.281
$\theta$ range, deg	3.11-27.48	3.09-27.48
no. of reflcns collected	5902	9366
no. of unique reflcns	2695	2238
<i>R</i> (int)	0.0496	0.0402
Good-of-fit on F <sup>2</sup>	1.020	1.086
<i>R</i> <sub>1</sub> [ <i>I</i> > 2σ( <i>I</i> )]	0.0620	0.0530
<i>wR</i> <sub>2</sub> [ <i>I</i> > 2σ( <i>I</i> )]	0.1218	0.1571
<i>R</i> <sub>1</sub> (all data)	0.1400	0.0684
<i>wR</i> <sub>2</sub> (all data)	0.1477	0.1675

1. Gao, B.-R., et al., Time-Resolved Fluorescence Study of Aggregation-Induced Emission Enhancement by Restriction of Intramolecular Charge Transfer State. *J. Phys. Chem. B* **2010**, *114*, 128-134.
2. Gao, B.-R., et al., Comparative Time-Resolved Study of Two Aggregation-Induced Emissive Molecules. *J. Phys. Chem. C* **2011**, *115*, 16150-16154.